Article

Chemistry & Biology

Characterization of the Biosynthetic Gene Cluster for Benzoxazole Antibiotics A33853 Reveals Unusual Assembly Logic

Graphical Abstract

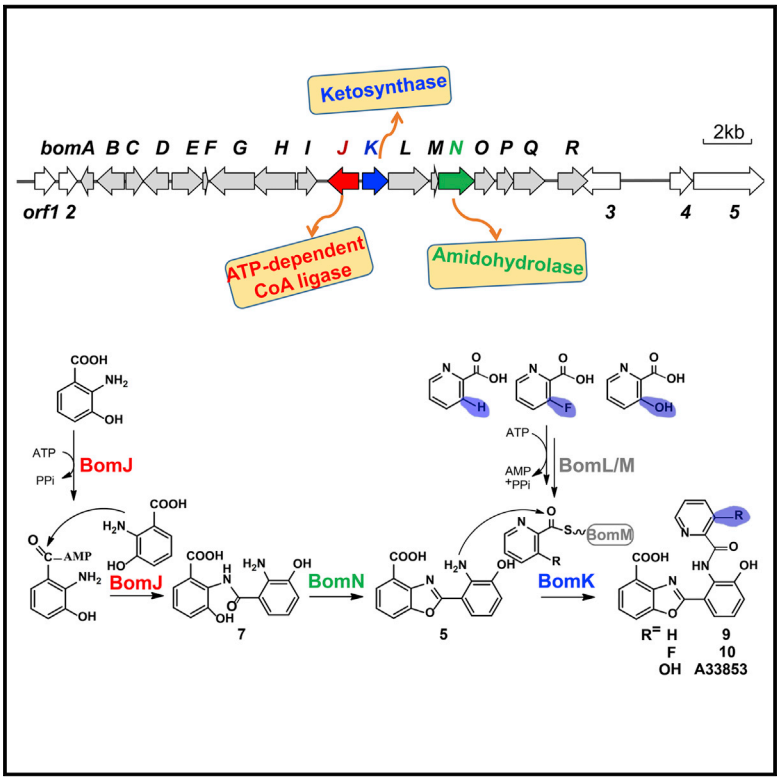

Authors

Meinan Lv, Junfeng Zhao, Zixin Deng, Yi Yu

Correspondence

yu_yi@whu.edu.cn

In Brief

Lv et al. unveil the pathway that directs the biosynthesis of the promising anti-leishmanial drug lead A33853, characterize a group of unusual enzymes responsible for the skeleton assembly of A33853, and generate two analogs of A33853 via mutasynthesis.

Highlights

- A group of interesting enzymes convert lysine into 3-hydroxypicolinic acid
- BomK is an unusual ketosynthase responsible for amide bond formation
- Enzymes putatively responsible for benzoxazole formation were identified
- Compounds with anti-leishmanial activity comparable with miltefosine biosynthesized

Accession Numbers

KR476659

Lv et al., 2015, Chemistry & Biology 22, 1313–1324
October 22, 2015
http://dx.doi.org/10.1016/j.chembiol.2015.09.005

Chemistry & Biology
Article

Characterization of the Biosynthetic Gene Cluster for Benzoxazole Antibiotics A33853 Reveals Unusual Assembly Logic

Meinan Lv,[1] Junfeng Zhao,[1] Zixin Deng,[1] and Yi Yu[1,*]
[1]Key Laboratory of Combinatory Biosynthesis and Drug Discovery (Ministry of Education), School of Pharmaceutical Sciences, Wuhan University, 185 East Lake Road, Wuhan 430071, P. R. China
*Correspondence: yu_yi@whu.edu.cn
http://dx.doi.org/10.1016/j.chembiol.2015.09.005

SUMMARY

A33853, which shows excellent bioactivity against *Leishmania*, is a benzoxazole-family compound formed from two moieties of 3-hydroxyanthranilic acid and one 3-hydroxypicolinic acid. In this study, we have identified the gene cluster responsible for the biosynthesis of A33853 in *Streptomyces* sp. NRRL12068 through genome mining and heterologous expression. Bioinformatics analysis and functional characterization of the *orf*s contained in the gene cluster revealed that the biosynthesis of A33853 is directed by a group of unusual enzymes. In particular, BomK, annotated as a ketosynthase, was found to catalyze the amide bond formation between 3-hydroxypicolinic and 3-hydroxyanthranilic acid during the assembly of A33853. BomJ, a putative ATP-dependent coenzyme A ligase, and BomN, a putative amidohydrolase, were further proposed to be involved in the benzoxazole formation in A33853 according to gene deletion experiments. Finally, we have successfully utilized mutasynthesis to generate two analogs of A33853, which were reported previously to possess excellent anti-leishmanial activity.

INTRODUCTION

Leishmaniasis is one of the most neglected tropical diseases caused by several protozoan parasites belonging to the genus *Leishmania*, which are transmitted to humans through the bites of infected female sandflies. Leishmaniasis is currently prevalent in 98 countries, where 1.3 million new cases and 20,000 to 40,000 deaths are estimated to occur each year (Alvar et al., 2012). Moreover, about 350 million people are at risk of infection, and 1.7 billion people live in areas suitable for leishmaniasis transmission, which raises global health concern about this disease (Pigott et al., 2014; Salam et al., 2014).

Due to the slow rate of progress in vaccine development against *Leishmania*, current leishmaniasis control mainly relies on several non-specific drugs (Chappuis et al., 2007; Mutiso et al., 2013). Pentavalent antimonials, which are very toxic and show serious side effects including cardiac arrhythmia and acute pancreatitis, have been widely used as the first-line treatment for all kinds of leishmaniasis for more than 70 years (Chappuis et al., 2007). Recently, new anti-leishmanial agents, such as amphotericin B, miltefosine, and paromomycin, have been developed to replace antimonials gradually (Croft et al., 2006a). Despite their much better *Leishmania* inhibition effects compared with antimonials, these drugs are still far from satisfactory because of their high treatment cost, normal cell toxicity, side effects, and the emergence of drug resistance (Joshi et al., 2014). Hence, it is imperative to discover and develop new anti-leishmanial molecular scaffolds with improved bioactivity and lowered cytotoxicity (Chappuis et al., 2007; Croft et al., 2006a, 2006b).

Antibiotic A33853 (**1**, Figure 1) was isolated from the culture broth of *Streptomyces* sp. NRRL12068 three decades ago (Michel et al., 1984; Tipparaju et al., 2008). Early studies have shown that **1** exhibits broad-spectrum antibiotic/antiviral activity by inhibiting the growth of certain pathogenic microorganisms and a number of viruses (Michel et al., 1984). Recently, **1** has been found to possess potent anti-leishmanial activity, 3-fold more active than the oral drug miltefosine, which makes **1** and its analogs promising scaffolds for the development of novel anti-leishmanial drugs (Tipparaju et al., 2008).

Structurally, **1** contains an unusual benzoxazole-based scaffold composed of two molecules of 3-hydroxyanthranilic acid (3-HAA) and one unit of 3-hydroxypicolinic acid (3-HPA) (Figure 1). Several natural products including nataxazole (Sommer et al., 2008), UK-1 (Shibata et al., 1993), caboxamycin (Hohmann et al., 2009), and calcimycin (Reed and Lardy, 1972) also contain the same benzoxazole moiety found in **1** (Figure 1), which raises an interesting question of how this unusual moiety is constructed by nature in these compounds. In the biosynthesis of calcimycin, 3-HAA has been demonstrated to condense with CalA4-tethered polyketide chain to form the direct precursor of the benzoxazole ring (Wu et al., 2011). Recently, Olano and coworkers identified the biosynthetic pathway of nataxazole, in which the biosynthesis of benzoxazole moiety was suggested to follow a similar condensation reaction between NatAC1-tethered 6-methylsalicylic acid (6-MSA) and NatAC2-tethered 3-HAA (Cano-Prieto et al., 2015). In both aforementioned cases, an acetalization reaction has been proposed to be essential for the generation of the benzoxazole ring. However, no enzyme(s) has been characterized for this role until now, and this remains the most important piece in the benzoxazole compounds biosynthesis puzzle.

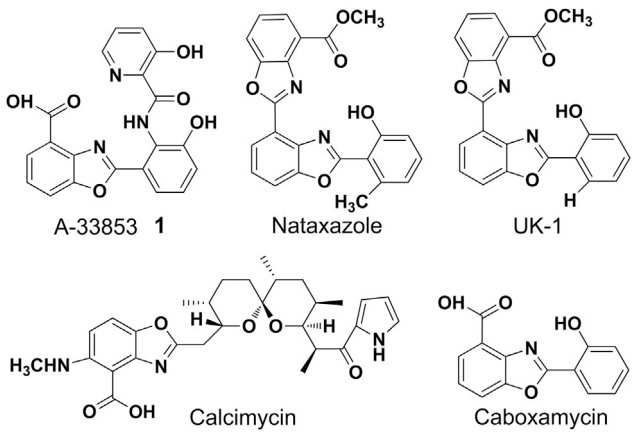

Figure 1. Structures of A33853 and Other Natural Products Containing a Benzoxazole Moiety

While **1** provides such an excellent lead for anti-leishmanial activity, it is often essential to generate analogs with improved physicochemical properties (Tipparaju et al., 2008). One expeditious approach is through combining the harnessed biosynthetic pathway with mutasynthesis. The biosynthesis of **1** must first be understood to achieve this.

Here, we report the identification and characterization of the gene cluster responsible for the biosynthesis of **1** in *Streptomyces* sp. NRRL12068. Biochemical characterization of the putative ketosynthase BomK demonstrates that it catalyzed the amide bond coupling between 3-HAA and 3-HPA. Through gene deletion experiments, we then revealed that BomJ and BomN, a putative ATP-dependent coenzyme A (CoA) ligase and a putative amidohydrolase, respectively, may be involved in the assembly of the benzoxazole ring in **1**. With the disclosure of the assembly logic of **1**, we further generated two analogs of **1**, which were reported previously to possess anti-leishmanial activity comparable with that of miltefosine, by employing the strategy of mutasynthesis in Δ*bomE* mutant.

RESULTS

Identification of the A33853 Biosynthetic Gene Cluster in *Streptomyces* sp. NRRL12068

Based on the observation that **1** and calcimycin share the same benzoxazole moiety (Figure 1), we speculated that the 3-HAA units in both compounds may have the same origin. In calcimycin biosynthesis, three enzymes (encoded by *calB1* through *calB3*) are involved in the conversion of chorismate to 3-HAA via the shikimate pathway (Wu et al., 2011). Thus, these gene products could be used as baits to identify the A33853 biosynthetic gene cluster. To this end, *Streptomyces* sp. NRRL12068 was subjected to Illumina genome sequencing (see Experimental Procedures). A homolog search of CalB1-B4 in the annotated genome of *Streptomyces* sp. NRRL12068 revealed a putative gene cluster encoding 4 open reading frames (ORFs) (BomO–BomR) that share high sequence similarity to CalB1–CalB4 (Figure 2A; Table S1). To verify the correlation of this gene cluster with A33853 production in *Streptomyces* sp. NRRL12068, *bomO* (the homologous gene of *calB3*) was inactivated. High-performance liquid chromatography (HPLC) analysis showed that the production of **1** was completely abolished in the extract of the *bomO* deletion mutant (WDY211, Figure 3), suggesting that the identified gene cluster may be involved in the biosynthesis of **1**.

Heterologous Expression of the A33853 Biosynthetic Gene Cluster in *Streptomyces albus*

To further determine whether the identified gene cluster is responsible for the biosynthesis of **1**, we constructed a genomic library of *Streptomyces* sp. NRRL12068 using an integrative *Streptomyces-Escherichia coli* shuttle vector, pJTU2554 (Li et al., 2008). A PCR-based scanning using *bomO* as a probe was performed to obtain a cosmid 8D3, which covers ~35 kb of the chromosome region spanning from *orf1* to *orf4* (Figure 2A). Cosmid 8D3 was then introduced into *Streptomyces albus* J1074 to generate the recombinant strain WDY200. Comparison of the HPLC profile between the ethyl acetate extracts of WDY200 and the control *S. albus* strain (WDY502, containing an empty vector) revealed one distinct peak in the extract of WDY200, which had the same retention time with the peak of **1** in the extract of *Streptomyces* sp. NRRL12068 (Figure 2B). This peak was further characterized through high-resolution electrospray ionization mass spectrometry (HR-ESIMS), which gave an ion with the same mass as protonated **1** (*m/z* 392.0880 $[M + H]^+$, calculated 392.0877 $[M + H]^+$, Figure 2C). Tandem MS (MS/MS) analysis also indicated that the fragmentation pattern of the peak matches exactly that of **1** from *Streptomyces* sp. NRRL12068 (Figure 2C). Taken together, these results demonstrate that the identified gene cluster in cosmid 8D3 is responsible for the production of **1**, and henceforth we named this gene cluster *bom*.

Determination of the A33853 Gene Cluster Boundaries

To determine the minimal contiguous gene cluster required for the biosynthesis of **1**, we inactivated a series of *orf*s at both sides of the region covered by cosmid 8D3 in NRRL12068 through in-frame deletion. On the left side, deletion of *orf2* had no effect on the production of **1** (Figure 2B), suggesting that this gene is located outside the *bom* cluster. In contrast, deletion of *bomB* completely abolished the production of **1** in the mutant strain WDY204, confirming that this gene is essential for the biosynthesis of **1** (Figure 2B). Because many efforts to knock out *bomA* in *Streptomyces* sp. NRRL12068 failed, we then removed *bomA* from the cosmid 8D3 by targeted in-frame deletion, and introduced 8D3Δ*bomA* into *S. albus* for heterologous expression. HPLC analysis of the ethyl acetate extract of the recombinant strain WDY223 showed that production of **1** was completely abolished in this strain compared with WDY200 (Figure 2B), thus confirming that *bomA* is the upstream border of the *bom* cluster. On the right side, deletion of *orf3* led to no change in the metabolic profile of the resultant mutant strain WDY213, while the production of **1** decreased in the Δ*bomR* mutant strain WDY212 compared with that in the wild-type strain (Figure 2B), indicating that *bomR* marks the downstream border of the *bom* cluster.

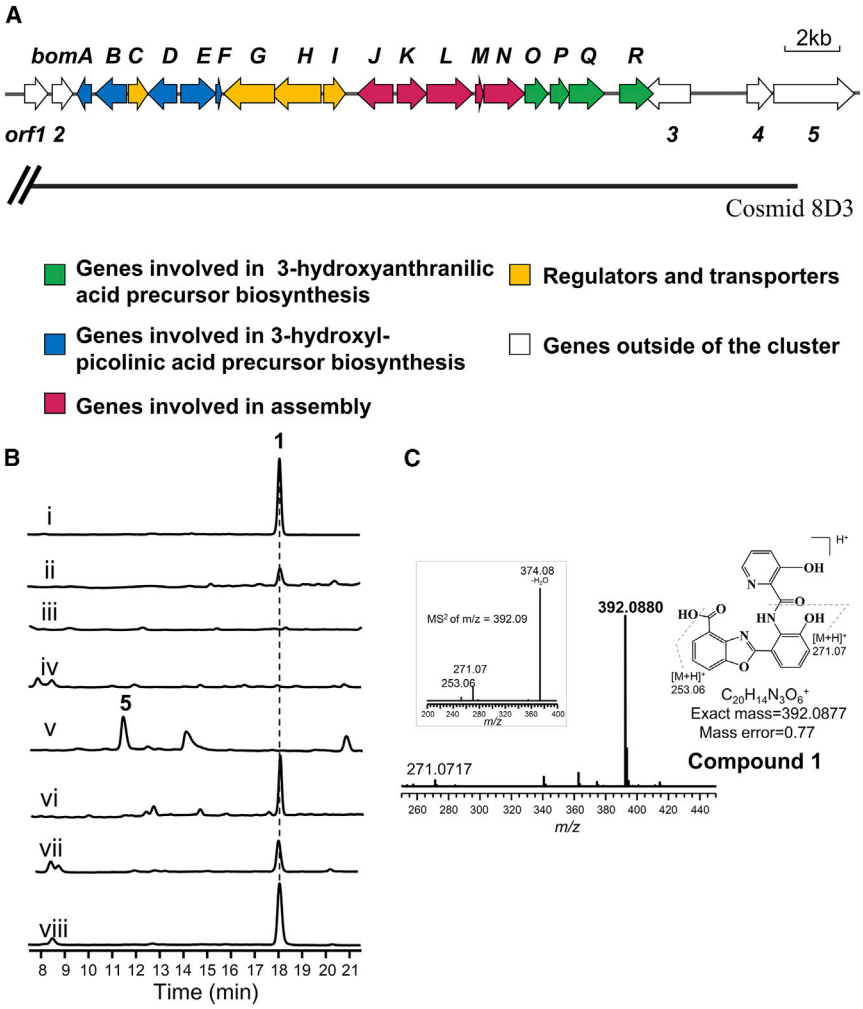

Figure 2. Identification of A33853 Biosynthetic Gene Cluster

(A) Genetic organization of the A33853 biosynthetic gene cluster. The deduced functions of each gene are labeled in color and summarized in Table S1.

(B) HPLC analysis of the heterologous expression of 8D3 in *Streptomyces albus*, and determination of the boundaries of the *bom* gene cluster. HPLC analysis of the metabolites of (i) wild-type *Streptomyces* sp. NRRL12068; (ii) *S. albus*::8D3 (WDY 200); (iii) *S. albus*::empty vector pJTU2554 (WDY502); (iv) *S. albus*::8D3Δ*bomA* (WDY223); (v) Δ*bomB* mutant WDY204; (vi) *orf2* in-frame deletion mutant WDY202; (vii) Δ*bomR* mutant WDY212; and (viii) *orf3* in-frame deletion mutant WDY213. UV monitored at 254 nm.

(C) HR-ESIMS/MS analysis of compound **1**.

In Silico and Functional Analysis of the Genes Involved in A33853 Biosynthesis

Based on the sequence analysis of the deduced products of each gene in the *bom* cluster (Table S1), these genes can be classified into four groups.

Genes Putatively Involved in the Biosynthesis of 3-HAA

Four genes, *bomO* to *bomR*, are identified in the *bom* cluster to encode proteins that show high similarity to those (CalB1–CalB4 and NatAL–NatDB) involved in the biosynthesis of 3-HAA moiety in calcimycin and nataxazole pathway, respectively (Table S1) (Cano-Prieto et al., 2015; Wu et al., 2011). The gene *bomR* encodes a putative 3-deoxy-D-arabino-heptulosonic acid 7-phosphate (DAHP) synthase, which may catalyze the condensation of phosphoenolpyruvate and erythrose-4-phosphate to form DAHP, the precursor for the following chorismate biosynthesis. BomQ, a putative anthranilate synthase, may catalyze the addition of ammonia from glutamine to C2 of chorismate to generate 2-amino-2-desoxyisochorismate, which is further hydrolyzed by BomP, a putative isochorismatase, to remove the vinyl ether functional group to yield 2,3-dihydro-3-hydroxyanthranilic acid (DHHA). The gene product of *bomO* is a putative 2,3-dihydro-2,3-dihydroxybenzoate dehydrogenase, which is possibly involved in the oxidation of DHHA to afford 3-HAA. Taken together, *bomO–bomR* constitute a gene cassette responsible for the supply of 3-HAA moiety for the assembly of **1** (Scheme 1A).

Genes Putatively Involved in the Biosynthesis of 3-HPA

The gene product of *bomE* resembles the L-lysine 2-aminotransferase VisA from *Streptomyces virginiae* (63% identity), which has been characterized in vitro to convert L-lysine into Δ^1–piperidine 2-carboxylic acid by transamination of the 2-amino group of the substrate (Namwat et al., 2002). To clarify its function, we deleted the gene *bomE* in-frame, yielding the Δ*bomE* mutant WDY201. HPLC analysis indicated that WDY201 completely abolished the production of **1** but accumulated two new compounds (**2** and **5**, Figure 3). The chemical formula of **2** was determined by HR-ESIMS to be $C_{21}H_{15}O_2N_5^+$ (*m/z* 375.0969 $[M + H]^+$, calculated 375.0976, Figure 4A). Further MS/MS analysis of **2**'s fragmentation pattern suggested that it has the same structure as **1**, except for the 3-HPA moiety being substituted by the benzoic acid (Figure 4A). The structure of **5** was revealed to differ from **1** by lacking the 3-HPA unit through nuclear magnetic resonance (NMR) analysis including ^1H, ^{13}C, correlation spectroscopy (COSY), heteronuclear single-quantum coherence, and heteronuclear multiple-bond correlation (HMBC) (Figures 4B and S1). These results suggested that BomE is responsible for the biosynthesis of 3-HPA, and other building block(s) (i.e. benzoic acid) in addition to 3-HPA could also be recognized by *bom* machineries and incorporated into **1**'s assembly line in the Δ*bomE* mutant. To further investigate the lysine aminotransferase activity, we expressed and purified to homogeneity the recombinant protein BomE from *E. coli*. The biochemical reactions were monitored according to the method developed previously (Soda et al., 1968). Liquid chromatography (LC)-MS analysis showed that both L-lysine and D-lysine can be converted by BomE to generate Δ^1-piperidine 2-carboxylate, which reacted specifically with aminobenzaldehyde (**4**) to give compound **3**,

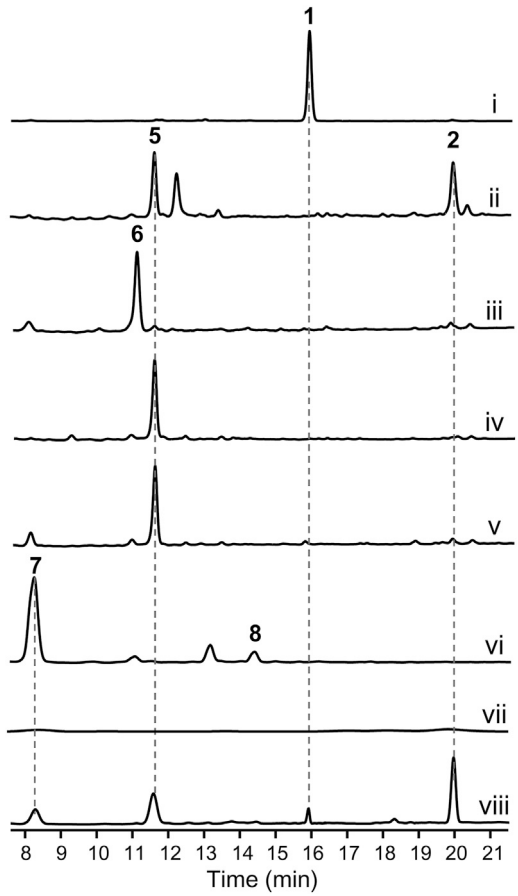

Figure 3. HPLC Analysis of Metabolite Profiles of the *bom* Gene In-Frame Deletion Mutants

(i) Wild-type *Streptomyces* sp. NRRL12068; (ii) Δ*bomE* mutant WDY201; (iii) Δ*bomJ* mutant WDY207; (iv) Δ*bomK* mutant WDY208; (v) Δ*bomL* mutant WDY209; (vi) Δ*bomN* mutant WDY210; (vii) Δ*bomO* mutant WDY211; and (viii) WDY211 fed with compound **7**. UV monitored at 254 nm.

while no transformation of L/D-lysine took place when heat-inactivated BomE was used in the control reaction (Figure S2). This finding definitely supports the proposed pathway in Scheme 1B that lysine is the precursor for biosynthesis of 3-HPA.

There are three *orf*s in *bom* gene cluster possibly involved in the following oxidation tailoring on Δ^1-piperidine 2-carboxylic acid. The gene *bomB* encodes a putative oxidoreductase in the *bom* gene cluster, which might be responsible for the aromatization of Δ^1-piperidine 2-carboxylic acid to give picolinate (Scheme 1B). One support for this hypothesis is that BomB shares 40% sequence similarity with NikD that has been characterized to catalyze an unusual four-electron oxidation reaction to transform Δ^1-piperideine-2-carboxylate to picolinate in the biosynthesis of nikkomycin (Bruckner et al., 2004; Venci et al., 2002). Moreover, as mentioned above, production of **1** was blocked in the Δ*bomB* mutant strain WDY204. However, this mutant could also accumulate a new compound whose identity was confirmed to be the same as **5** (Figures 2B and 4B). These results further support the proposed pathway directing the biosynthesis of 3-HPA.

The gene product of *bomD* is a putative flavin-dependent oxidoreductase displaying similarity with TgaE from *Sorangium cellulosum* (30% identity, 45% similarity). Given that TgaE is a functional flavin-dependent hydroxylase responsible for the C-17 hydroxylation in the biosynthesis of Soce-thuggacin B (Buntin et al., 2010), BomD is possibly involved in the C-3 hydroxylation of picolinate (Scheme 1B). The gene *bomA* encodes a putative nicotinamide adenine dinucleotide (NADH):flavin mononucleotide (FMN) oxidoreductase, which shows high similarity to Med-orf13 (53% identity) from *Streptomyces* sp. AM-7161 (Ichinose et al., 2003), SnaC (51% identity) from *Streptomyces pristinaespiralis* (Blanc et al., 1995), and ActVB (39% identity) from *Streptomyces coelicolor* A3(2) (Kendrew et al., 1995). All of these proteins belong to the two-component monooxygenase system, which is generally involved in catalyzing the reduction of FMN by NADH and supplying the reduced flavin to other monooxygenase(s) for the subsequent oxidation of various substrates (Ellis, 2010; Sucharitakul et al., 2014). Thus, BomA may act as the $FMNH_2$-supplying partner enzyme with BomD.

Interestingly, we also found a very small *orf bomF*, which locates immediately downstream of *bomE*. BomF is a putative tautomerase belonging to 4-oxalocrotonate tautomerase family, members of which have been characterized to be involved in the conversion of 2-hydroxymuconate to 2-oxo-3-heedioate in a catabolic pathway for aromatic hydrocarbons (Burks et al., 2010; Wang et al., 2007). The exact function of BomF in the biosynthesis of **1** remains to be determined.

Genes Putatively Involved in the Assembly of 1

The *bom* cluster contains two genes, *bomL* and *bomM*, which encode proteins with high sequence similarity to PyrA (61% identify), a 3-HPA:AMP ligase, and PyrU (32% identity), the phosphopantetheine-binding protein in the biosynthesis of pyridomycin (Huang et al., 2011), respectively. The Δ*bomL* mutant WDY209 completely lost the production of **1** but accumulated a new compound with the same retention time as **5** produced by WDY201 (Figure 3). HR-ESIMS analysis of the compound showed an $[M + H]^+$ ion at *m/z* 271.0713, thus confirming the identity of the compound as **5** (Figure 4B). This result suggested that activation of 3-HPA is required before this moiety could be incorporated into the assembly line of **1**. To confirm the functions of BomL and BomM, we performed the enzyme assays of these two proteins in vitro. The recombinant BomL was then overexpressed in *E. coli* and purified to homogeneity, while BomM was overexpressed in *E. coli* together with Sfp to ensure the complete conversion of the *apo* form of BomM to its corresponding *holo* form. The reaction was set up by incubating the substrate 3-HPA with both BomL and *holo*-BomM in a buffer containing Mg^{2+}, ATP, and DTT. HR-ESIMS analysis showed that a new peak appeared at *m/z* 12268.1 Da, which corresponds to the molecular ion for 3-HPA-BomM (calculated 12,269.1 Da) (Figure 5C), consistent with the activation and transfer of 3-HPA to *holo*-BomM catalyzed by BomL.

Immediately upstream of *bomL* is located the gene of *bomK*, which encodes for a putative β-ketoacyl-acyl carrier protein (ACP) synthase (KSIII-like protein). Enzymes in this family are usually involved in the biosynthesis of polyketide natural products. To examine the function of BomK, we carried out the

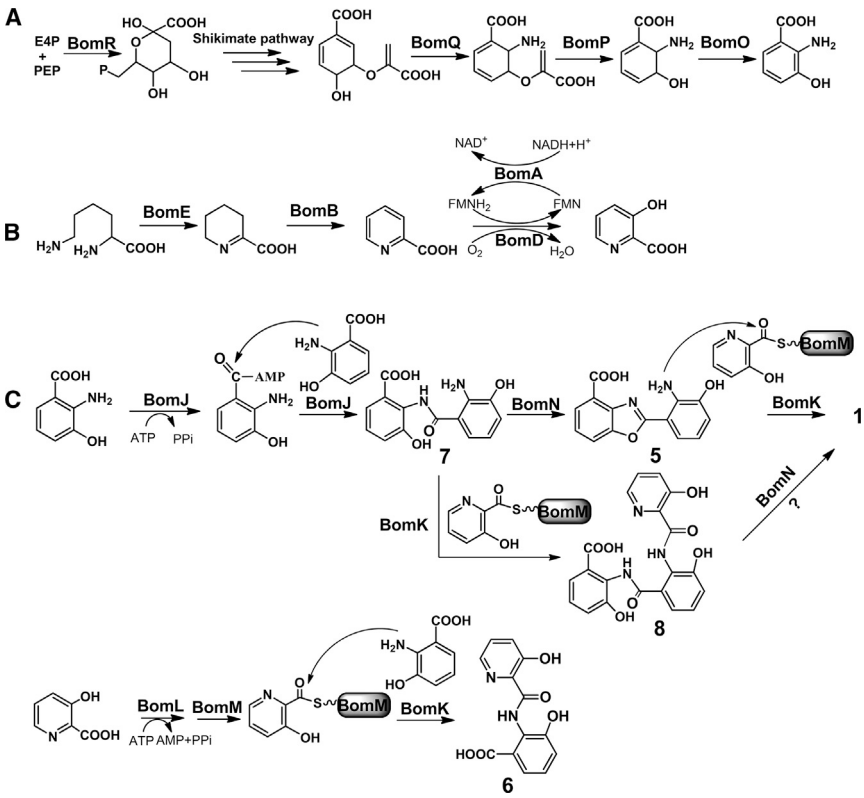

Scheme 1. The Proposed Biosynthetic Pathway of A33853

(A) Biosynthesis of 3-HAA.

(B) Biosynthesis of 3-HPA.

(C) Putative assembly line of A33853.

in-frame deletion of *bomK* in *Streptomyces* sp. NRRL12068. HPLC monitoring of the fermentation culture of the Δ*bomK* mutant WDY208 showed that the formation of **1** was completely abolished (Figure 3) and, unexpectedly, compound **5** was accumulated as determined by HR-ESIMS and MS/MS fragmentation analysis. We thus speculated that BomK may catalyze the amide bond formation between the amino group of the 3-HAA and the carbonyl group of the BomM-tethered 3-HPA (Scheme 1C). To demonstrate the exact function of BomK, the N-terminal small ubiquitin-related modifier (SUMO)-tagged BomK was produced in *E. coli* and the cell-free extract (CFE) of the recombinant *E. coli* was subjected to enzyme assay in vitro. The reaction of BomL/BomM with 3-HPA (see above) proceeded for 30 min, followed by addition of compound **5** and BomK-CFE. Analysis by LC coupled with HR-ESIMS observed the formation of **1** as evidenced by the exact mass and the same HPLC retention time as the authentic **1** (Figure 5D). In control experiments when assays were conducted with the CFE of the wild-type *E. coli*, there was no appearance of **1**. These results clearly verified that BomK is responsible for the amide bond formation between 3-HPA and 3-HAA during the biosynthesis of **1**.

The gene *bomN* encodes a putative amidohydrolase. To verify in vivo function of *bomN*, we constructed a mutant strain, WDY210, in which *bomN* was deleted in-frame. To our surprise, HPLC analysis indicated that WDY210 completely lost the production of **1** but accumulated two compounds (**7** and **8**, Figure 3). The structure of **7** was further determined through the interpretation of 1D and 2D NMR spectra (Figure S3). Although **8** could not be isolated, its mass is consistent with the predicted structure of **8** as deduced from the HR-ESIMS and MS/MS analysis (Figure 4). Both compounds lack the oxazole moiety compared with **5** and **1**, which implies that BomN may catalyze the heterocyclization reaction to afford the benzoxazole ring. To exclude the possibility of whether compound **7** accumulated in WDY210 is a shunt product, it was then fed to the fermentation culture of WDY211 in which the supply of 3-HAA is interrupted (Figure 3). As expected, WDY211 could convert **7** into **1**, **2**, and **5** (Figure 3), confirming that **7** is a true intermediate resulting from the inactivation of *bomN*. Although the catalytic mechanism of BomN still remains enigmatic at present, these results unambiguously characterize that **7** is the direct precursor of benzoxazole biosynthesis.

The accumulation of compound **8** in Δ*bomN* mutant led us to speculate that it may be generated by coupling of **7** and 3-HPA-BomM catalyzed by BomK (Scheme 1C). To verify this assumption, we incubated **7** with BomK-CFE in the assay system in the same way as for **5**. LC-HR-ESIMS clearly showed the production of **8** in the reaction sample compared with the control (Figure 5D). These data suggest that both **5** and **7** could be recognized by BomK. However, we cannot determine whether **8** is a shunt product or an alternative precursor for the biosynthesis of **1** at present.

The gene product of *bomJ* shows high sequence similarity to coenzyme F390 synthetase or phenylacetate-CoA ligase. Enzymes belonging to this family usually catalyze an ATP-dependent adenylation of a carboxylate substrate to its corresponding thiolated form. BomJ shares 36% identity and 46% similarity with YtkQ, which has been characterized as an ATP-dependent CoA ligase involved in the activation of the carboxyl group of the precursor for the subsequent amide bond formation in the biosynthesis of yatakemycin (Huang et al., 2012). BomJ may activate 3-HAA similarly to the AMP-linked intermediate, and then direct nucleophilic attack of the amino group of one 3-HAA to the acyl group of AMP-linked 3-HAA to afford **7** (Scheme 1C). Gene deletion of *bomJ* resulted in the complete loss of the production of **1** in the Δ*bomJ* mutant WDY207. Unexpectedly, a new compound was accumulated in WDY207 (Figure 3), and its structure was further deduced as **6** (*m/z* 275.0659 $[M + H]^+$, calculated 275.0663) through HR-ESIMS and MS/MS analysis (Figure 4). Compound **6** differs from **1** by consisting of a single 3-HAA unit connected with 3-HPA via an amide bond. One reasonable explanation for the production of **6** is that BomK displays substrate promiscuity

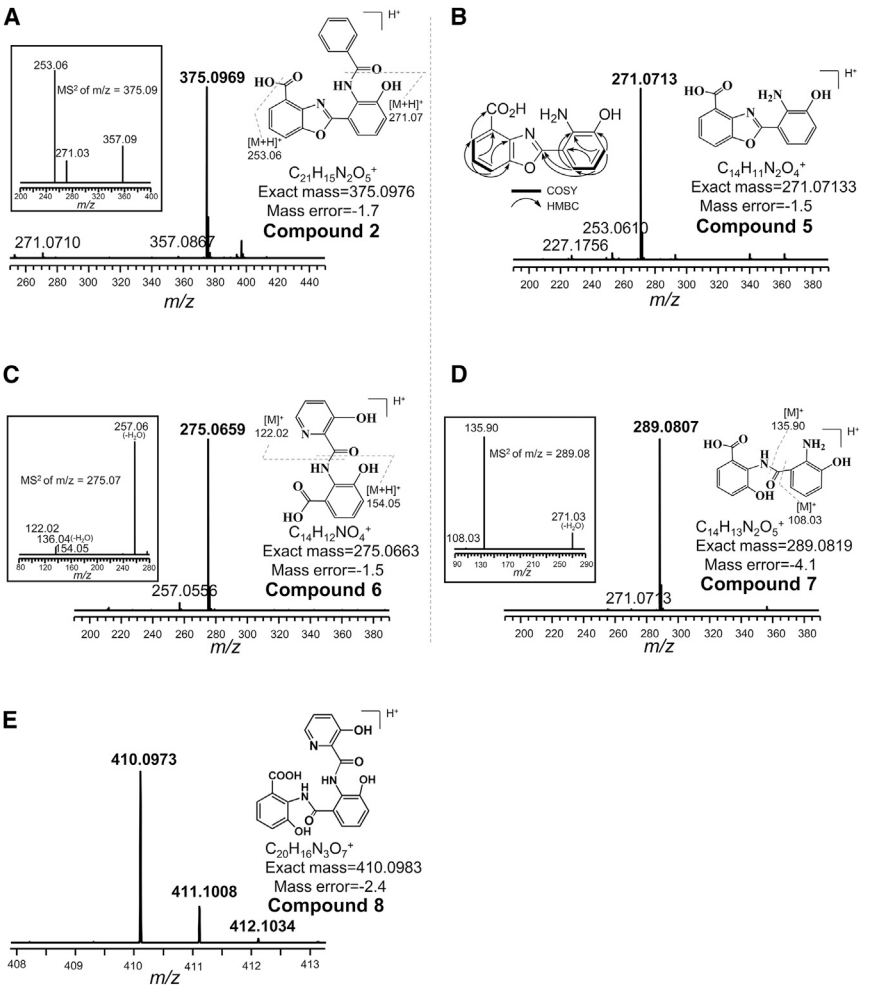

Figure 4. LC-HR-ESIMS Analysis of Compounds 2, 5, 6, 7, and 8

(A) LC-HR-ESIMS/MS analysis of compound **2.**

(B) LC-HR-ESIMS analysis of compound **5**. ^{1}H-^{1}H COSY and selected HMBC correlations are labeled in compound **5**.

(C) LC-HR-ESIMS/MS analysis of compound **6**.

(D) LC-HR-ESIMS/MS analysis of compound **7**.

(E) LC-HR-ESIMS analysis of compound **8**.

and catalyzes the coupling of free-standing 3-HAA with BomM-tethered 3-HPA.

Regulatory and Resistance Genes

The deduced product of *bomC* showed similarity to VmsS (44% identity), which is a pathway-specific transcriptional regulator in the virginiamycin biosynthetic pathway (Pulsawat et al., 2007), suggesting the possibility that BomC might positively regulate the biosynthesis of **1**. BomI resembles TetR family regulators, which contains a conserved helix-turn-helix DNA-binding domain pfam00440 (Ramos et al., 2005), implying that this protein may be a repressive transcriptional regulator. Consistent with this speculation, inactivation of *natR3*, the homologous gene of *bomI* (52% identity and 64% similarity) in the nataxazole pathway, led to 4-fold elevated nataxazole production (Cano-Prieto et al., 2015). Two putative transporter genes are also present in the *bom* cluster. The deduced amino acid sequence of *bomG* and *bomH* are highly similar to that of ATP-binding cassette transporters, which comprise a large and diverse group of proteins capable of transporting a wide variety of different compounds at the expense of ATP hydrolysis (Martin et al., 2005). In addition, BomG and BomH show high similarity with NatT1 and NatT2 from the nataxazole biosynthetic pathway (Table S1), respectively, implying that a similar self-protection mechanism may be utilized by A33853 and nataxazole-producing strains.

Mutasynthesis of A33853 Analogs in Mutant *Streptomyces* sp. NRRL12068

In an effort to design and develop novel anti-leishmanial agents, Tipparaju et al. (2008) synthesized **1** and several of its derivatives to evaluate their activities against leishmaniases. Compounds **9** and **10**, in which the 3-HPA moiety was substituted by picolinic acid and 3-fluoropicolinic acid, respectively, were thus found to display anti-leishmanial activity comparable with that of the first-line drug miltefosine while showing lower toxicity. Elucidation of the biosynthetic pathway of **1** provides us the opportunity to generate libraries of **1′** analogs for structure-activity relationship studies and even for the screening of promising anti-leishmanial drug candidates.

The accumulation of compound **2** in WDY201, together with the finding that inactivation of *bomK* led to the production of compound **5**, implied that BomK could accept substrates other than 3-HPA to assemble the analogs of **1**. We therefore set out to feed WDY201 with various substrates structurally similar to 3-HPA. As shown in Figure 6, the feeding of picolinic acid and 3-fluoropicolinic acid led to the production of two new compounds in WDY201 with $[M + H]^+$ ions at *m/z* 376.0922 and *m/z* 394.0824, respectively. MS/MS analysis of both ions' fragments further confirmed that these two compounds are **9** and **10**, respectively. However, several other substrates such as pyrimidine-2-carboxylic acid were also tested, but no corresponding analogs of **1** were detected in WDY201 (Figure 6), implying that these substrates may be toxic to the host strain or that these compounds could not penetrate into the cell, or that BomL/BomK could not accept these compounds as its substrates. Nevertheless, our findings open a new avenue for the development of novel pharmaceutical agents against *Leishmania*.

DISCUSSION

In this study, we have cloned the gene cluster for the biosynthesis of **1**, which contains an unusual benzoxazole moiety. Bioinformatics analysis and functional characterization of the *orf*s contained in the gene cluster led us to propose the biosynthetic pathway of **1** in *Streptomyces* sp. NRRL12068 as shown in Scheme 1.

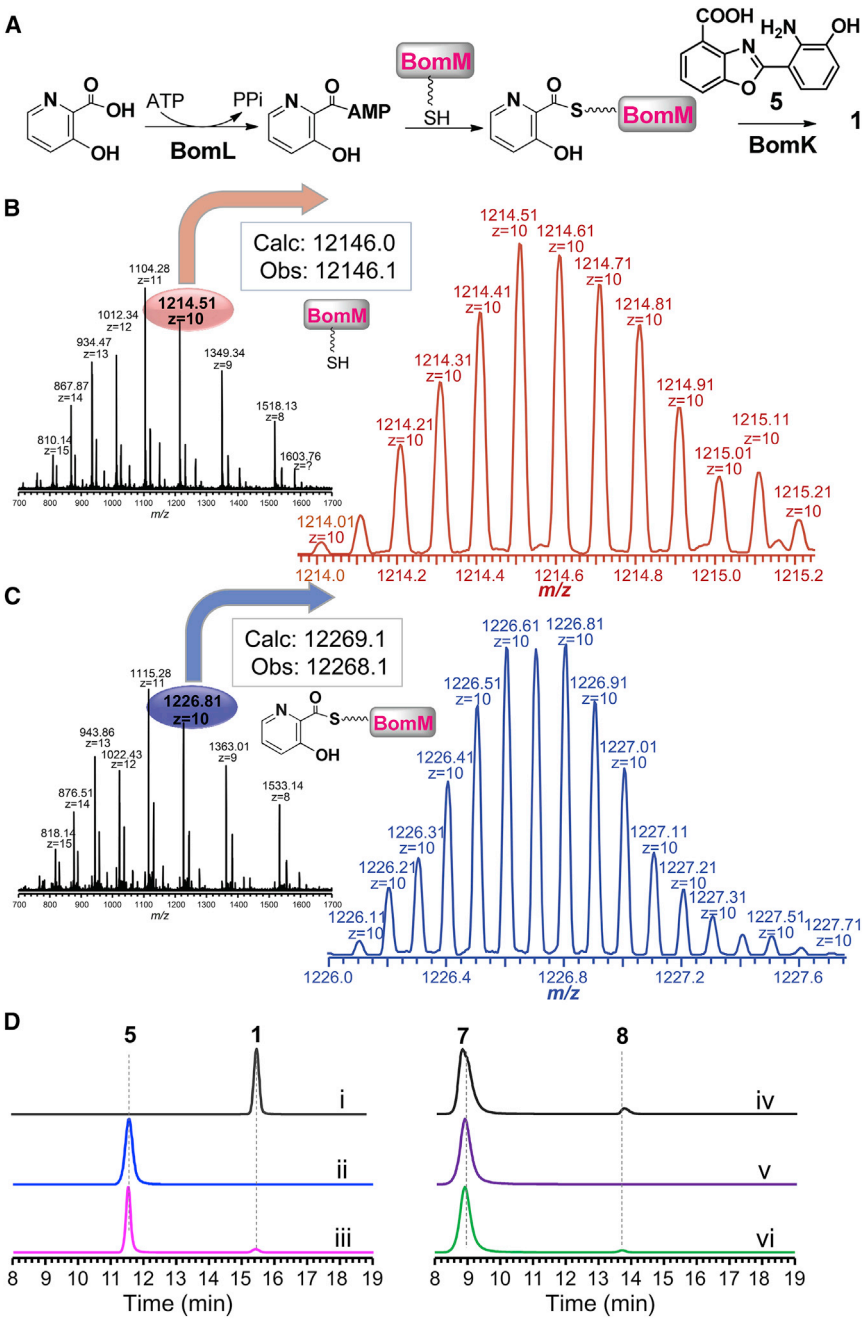

Figure 5. In Vitro Characterization of BomL, BomM, and BomK

(A) A scheme for BomL catalyzed reaction.

(B) HR-ESIMS analysis of *holo*-BomM in the control reaction without BomL.

(C) HR-ESIMS analysis of 3-HPA-*S*-BomM produced in BomL catalyzed reaction.

(D) LC-HR-ESIMS analysis of products of the BomK-CFE reactions. (i) Wild-type *Streptomyces* sp. NRRL12068; (ii) control assay with **5**; (iii) enzymatic conversion of **5** by BomK-CFE; (iv) Δ*bomN* mutant WDY210; (v) control assay with **7**; (vi) enzymatic conversion of **7** by BomK cell-free.

The 3-HPA residue has also been found in several other natural products including nikkomycin, virginiamycin, viridogrisein, and pyridomycin (Figure S4). Although the biosynthesis of picolinate, especially the steps involved in the aromatization of the piperidine ring, has been profoundly studied, little information is available for the hydroxylation reaction on the picolinic ring. In silico analysis indicated that the putative FMN reductase BomA and the putative flavin adenine dinucleotide-dependent oxidoreductase BomD may constitute a two-component flavin-dependent monooxygenase system to catalyze the hydroxylation on picolinic ring. Such two-component flavin-dependent monooxygenase systems are abundant in the biosynthetic pathways of natural products. For instance, ActVB has been characterized to form a two-component oxidation system with ActVA-ORF5 to catalyze the quinone forming at the C-6 of 6-deoxydihydrokalafungin, and hydroxylation at C-8 of dihydrokalafungin in the biosynthesis of actinorhodin (Okamoto et al., 2009; Taguchi et al., 2011, 2013; Valton et al., 2004, 2006). Another example is the two-component system composed of SnaA, SnaB, and SnaC, in which SnaC provides FMNH2 for the conversion of pristinamycin IIB to pristinamycin IIA catalyzed by the heterodimer of SnaA and SnaB (Blanc et al., 1995).

Peptide natural products are commonly assembled by three major strategies. The first one uses non-ribosomal peptide synthetase (NRPS) assembly lines to activate and condensate amino acid monomers in sequential order, as exemplified by the biosynthesis of vancomycin and daptomycin (Nolan and Walsh, 2009). The second employs the ribosomal synthesis machinery to yield a peptide precursor that will then undergo various posttranslational modifications and/or proteolysis to give the final product as exemplified by Microcin B17, thiopeptides, and the lantibiotics (Knerr and van der Donk, 2012; Nolan and Walsh, 2009; Zhang and Liu, 2013). The third strategy uses a group of ATP-dependent ligases to catalyze the coupling of amino acid monomers and accounts for the biosynthesis of novobiocin, coumermycin, and dapdiamide (Hollenhorst et al., 2009; Schmutz et al., 2003; Steffensky et al., 2000). Also, there are several uncommon strategies for the amide bond formation, such as the transglutaminase-like protein AdmF in the biosynthesis of andrimid, a putative class C β-lactamase CapW pair in the biosynthesis of A-503083s, and the tRNA-dependent aminoacyltransferase PacB in the biosynthesis of pacidamycin (Funabashi et al., 2010; Zhang et al., 2011). Another uncommon strategy in the natural product biosynthesis for amide bond formation is to use a free-standing substrate as the acceptor to

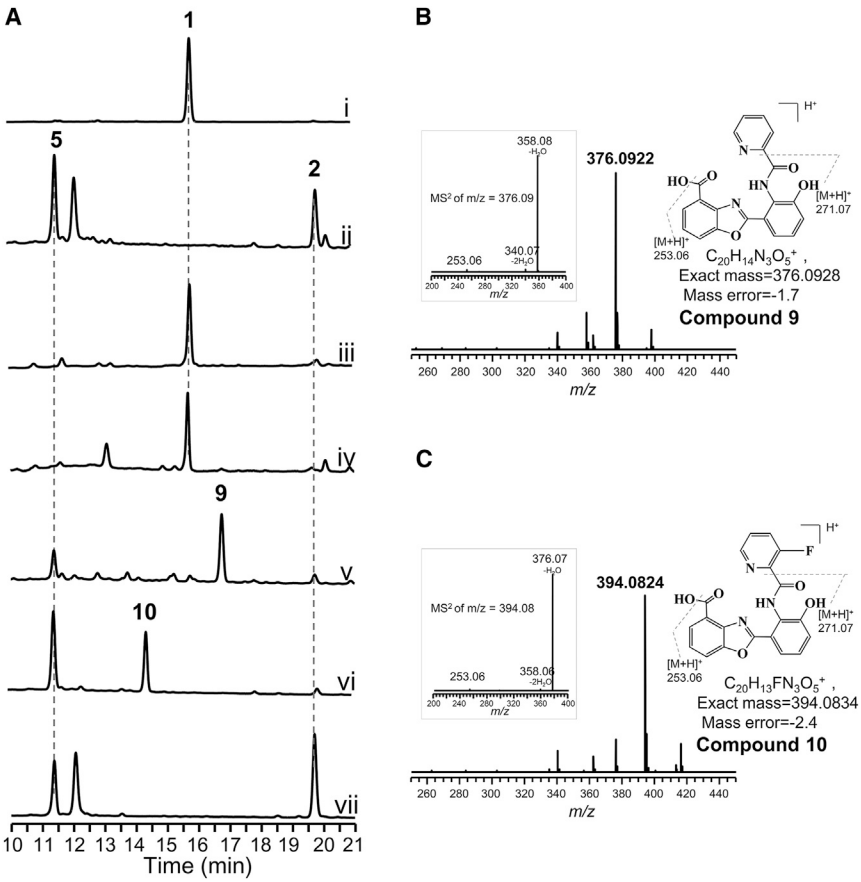

Figure 6. Mutasynthesis Performed in Δ*bomE* Mutant WDY201

(A) HPLC analysis of the metabolites of (i) wild-type *Streptomyces* sp. NRRL12068; (ii) Δ*bomE* mutant WDY201; (iii) Δ*bomE* complementation strain WDY214; (iv) WDY201 fed with 3-HPA; (v) WDY201 fed with picolinic acid; (vi) WDY201 fed with 3-F picolinic acid; and (vii) WDY201 fed with pyrimidine-2-carboxylic acid.

(B and C) LC-HR-ESIMS/MS analysis of compounds **9** (B) and **10** (C).

couple with a carrier protein-tethered acyl donor. One particular example can be found in the biosynthesis of vibriobactin whereby VibH, a free-standing C domain, was found to catalyze the formation of an amide bond (Keating et al., 2002). However, bioinformatics analysis of the *bom* cluster revealed none of the above amide synthase homologs. Instead, our study discovered an unprecedented case whereby the ketosynthase-like BomK catalyzes the amide bond formation in **1**'s pathway. Our data have shown that BomK could catalyze the transfer of BomM-tethered 3-HPA to the amino group of compounds **5** and **7**. In addition, the phylogenetic tree analysis of BomK and other ketosynthases revealed that it positions with ChlB3 and CerJ in the close clades (Figure S5), which implies that BomK functions like an acyl transferase (Bretschneider et al., 2012; He et al., 2009). Thus, this is the first report that a ketosynthase-like enzyme catalyzes the amide bond formation. It is highly likely that BomK also displays broad substrate tolerance and has the ability to convert BomM-tethered 3-HPA and free-standing 3-HAA into **6** (Scheme 1C).

We also deduced the function of BomJ as an amide bond synthetase that is responsible for the coupling of two units of 3-HAA. Sequence alignment of BomJ in GenBank showed that it belongs to the AFD superfamily by containing a conserved AMP-binding motif (SSGSAGQP). Enzymes in this superfamily generally activate a carboxylate substrate as an adenylate and then transfer the AMP-linked substrate to the pantetheine group of either CoA or acyl-carrier protein. We thus speculate that the proposed amide bond condensation activity of BomJ would resemble the catalysis performed by common CoA ligases, except that an amino group is used as the nucleophilic donor. A similar strategy has been proposed in the diazepinomicin pathway for amide bond formation catalyzed by a putative coenzyme F390 synthetase *orf24* (Bonitz et al., 2013). The in vitro biochemical characterization of BomJ, as well as genome mining of gene homologs of *bomK*/*bomJ* in other putative natural product biosynthetic gene clusters, which are currently under way in our laboratory, could shed light on understanding the novel enzymatic mechanisms for amide bond formation and discovering new a family of amide bond-containing natural products.

The structure of the oxazole heterocycle is unique in peptide natural products. Two enzymatic strategies have been evolved by nature to construct oxazole, one of which is directed by NRPS containing the Cy domain with the other being operated by the YcaO family of proteins (Melby et al., 2011). However, there is no homolog of these classic oxazole synthases found in the *bom* cluster. Unexpectedly, our results indicate that BomN, a putative amidohydrolase, is possibly responsible for the oxazole ring closure reaction, since two compounds lacking an oxazole ring were accumulated in Δ*bomN* mutant strain (Figures 3 and 4). The BomN-catalyzed reaction may thus represent the third enzymatic strategy to construct oxazole in nature. It is interesting to note that calcimycin also contains the same benzoxazole moiety, whose biosynthesis is still enigmatic (Wu et al., 2011). However, there is no homologous gene of *bomN* contained in the *cal* gene cluster, implying that diverse mechanisms directing the formation of benzoxazole exist.

Recently, Olano and coworkers proposed a model for the biosynthesis of nataxazole in *Streptomyces* sp. Tü6176 (Cano-Prieto et al., 2015). They speculated that all the building blocks, including 6-MSA and 3-HAA, were connected with each other via two amide bonds in the form of ACP (NatAC1 and NatAC2)-tethered intermediates during the biosynthesis of nataxazole. However, the enzymes responsible for the formation of the amide bonds and the benzoxazole were not identified. Nataxazole and **1** are very close in structure, implying that they share similar logic in skeleton assembly. In this work, we have determined the

enzyme (BomK) that is involved in amide bond formation between 3-HPA and 3-HAA via both in vivo and in vitro experiments, and proposed the functions of two other enzymes (BomJ and BomN) that may be responsible for the benzoxazole formation according to the gene knockout results. Our study thus provides further insights into the logic underlying the biosynthesis of natural products in the benzoxazole family.

SIGNIFICANCE

Antibiotic A33853 is a promising scaffold lead for the development of novel anti-leishmanial drugs. It contains an unusual benzoxazole moiety under which the formation mechanism is still enigmatic. In this work, we have identified and functionally characterized the individual genes involved in the biosynthesis of A33853. Our findings not only suggest an interesting logic underlying the skeleton assembly of A33853 in which an unusual ketosynthase-like enzyme BomK is involved in the amide bond formation between 3-HPA and 3-HAA, but also provide clues to understanding how benzoxazole is formed during the biosynthesis of such groups of natural products. In addition, the successful generation of two analogs of A33853 paves the way for further engineering of the discovered biosynthetic machinery to create new drug leads for anti-leishmanial agents.

EXPERIMENTAL PROCEDURES

Media and Strains

E. coli DH10B and *E. coli* ET12567 (pUZ8002) were cultured in L Broth or L agar at 37°C. *Streptomyces albus* J1074, *Streptomyces* sp. NRRL12068, and its related mutant were cultured on MS medium (20 g/l mannitol, 20 g/l soybean meal, 20 g/l agar, pH 7.2) for spores formation, in TSBY medium (5 g/l yeast extract, 30 g/l tryptone soya broth) for mycelium and seeds culture, and in AY medium (70 g/l dextrin, 10 g/l BD peptone, 4 g/l $MgSO_4{\bullet}7H_2O$, 5 g/l oatmeal, 5 g/l $CaCO_3$) for fermentation. MS medium containing the final concentration of 30 mM Mg^{2+} was used for conjugation of *S. albus* and *Streptomyces* sp. NRRL12068.

DNA Sequencing and Analysis

Streptomyces sp. NRRL12068 genomic DNA was prepared through the salting-out method, and sequenced by Illumina Hiseq 2000 with a 300-bp paired-end library by the TruSeq method. A total of 4,143,748 paired-reads were obtained and assembled by SOAP de novo software (http://soap.genomics.org.cn/soapdenovo.html) with the parameters "sequence length >25 bp and base quality >20." When the K-mer was 21, the best assembly result could be obtained. The resultant 165 scaffolds were further annotated by RAST (http://rast.nmpdr.org/rast.cgi) and further analysis via antiSMASH (http://antismash.secondarymetabolites.org). The A33853 biosynthetic gene cluster was identified from the sequenced genome via silica analysis, and was submitted to NCBI GenBank with the accession number GenBank: KR476659.

The ORFs were deduced from the sequence using the FramePlot 4.0 beta program (http://nocardia.nih.go.jp/fp4/). The corresponding deduced proteins were compared with other known proteins in the databases using BLAST (http://www.ncbi.nlm.nih.gov/blast/). Amino acid sequence alignments were performed with the CLUSTALW algorithm from BIOLOGYWORKBENCH 3.2 software (http://workbench.sdsc.edu).

Genomic Library Construction and Screening

A genomic library of *Streptomyces* sp. NRRL12068 was constructed using a Copy Control Fosmids Library Production Kit (Epicentre Biotechnologies Cat. No. CCFOS110) according to the manufacturer's instructions, except that the vector used was EcoRV-digested pJTU2554 instead of pCC1Fos. The primers (Primer-oxo-F/Primer-oxo-R, Primer-dam-F/Primer-dam-R, and Primer-pfa-F/Primer-pfa-F R) were used for PCR-based screening of the genomic library. Cosmid 8D3 was thus identified to contain the putative A33853 biosynthetic gene cluster.

Construction of WDY201 to WDY213

To inactivate *bomE*, a 2,245-bp upstream fragment and a 2,241-bp downstream fragment were amplified from cosmid 8D3 by PCR using the primers bomE-Left-F/bomE-Left-R and bomE-Right-F/bomE-Right-R, respectively. PCR was performed in 30 μl of volume with 5% DMSO and KOD DNA polymerase (Toyobo). The obtained fragments were digested with XbaI/BamHI and BamHI/EcoRI, respectively, and cloned into the XbaI/EcoRI site of pKC1139 to give the in-frame deletion construct pWDY201, which was then transferred into *Streptomyces* sp. NRRL12068 via *E. coli-Streptomyces* conjugation. Following the procedure described previously (Yu et al., 2009), the *bomE* in-frame deletion mutant strain was screened out and designated as WDY201. The same strategy was employed to construct WDY202 to WDY213, in which *orf2*, *bomB*, *bomC*, *bomD*, *bomJ*, *bomK*, *bomL*, *bomN*, *bomO*, *bomR*, and *orf3* were in-frame deleted from *Streptomyces* sp. NRRL12068, respectively.

Complementation of Gene Knockout Strains

To complement *bomE* knockout strain WDY201, a 1,294-bp fragment containing the whole *bomE* gene sequence was amplified by high-fidelity PCR using primers HB-bomE-F/HB-bomE-R. The obtained fragment was then cloned into the NdeI/EcoRI site of pIB139, which can integrate into *attB* site in *Streptomyces* chromosome, to generate the construct pWDY214. It was then transferred into WDY201 via *E. coli-Streptomyces* conjugation. Following the procedure described above, the Δ*bomE* complementation mutant strain was screened out and designated as WDY214. The same strategy was employed to construct WDY215 to WDY218, in which gene deletion of *bomO*, *bomB*, *bomC*, and *bomK* was complemented, respectively.

Cultivation, Fermentation, and LC-HRMS Analysis

Streptomyces sp. NRRL12068 and its related mutant strains were inoculated into TSBY medium and grown for 36 hr at 28°C at 220 rpm, then transferred into AY fermentation medium for continuous cultivation at 28°C and 220 rpm for 7 days. The culture was then centrifuged and the supernatants collected, which were further extracted by an equal volume of ethyl acetate. The organic phase was collected and evaporated to dryness. Residues were redissolved in 1/100 of original culture volume of methanol for HPLC or LC-MS detection. The HPLC analyses were carried out on a DIONEX system equipped with a P680 HPLC pump using a DIKMA Diamonsil C18 column (5 μm, 250 × 4.6 mm) eluted with a linear gradient from 60:40 A/B to 15:85 A/B over 15 min after balanced 5 min with 60:40 A/B at a flow rate of 0.8 ml/min (solvent A was 0.1% formic acid in H_2O and solvent B was 0.1% formic acid in CH_3CN). UV was monitored at 254 nm. The identities of A33853 and its analogs were characterized by high-resolution MS (HRMS) analysis, which consists of a full scan in positive mode followed by a data-dependent fragmentation scan, through a Thermo Scientific LTQ XL Orbitrap mass spectrometer equipped with a Thermo Scientific Accela 600 pump (Thermo Fisher Scientific). The following parameters were set: capillary voltage 45 V, capillary temperature 45°C, auxiliary gas flow rate 10 arbitrary units (a.u.), sheath gas flow rate 40 a.u., spray voltage 3.5 kV, and mass range 100–2000 amu (maximum resolution 30,000).

Mutasynthesis of Analogs of A33853 in *Streptomyces* sp. NRRL12068

For the mutasynthesis of analogs of A33853, 5 ml seed culture of WDY201 was inoculated into 50 ml AY fermentation broth after being grown at 28°C and 220 rpm for 36 hr. The final concentration of 100 μg/ml 3-HPA, picolinic acid, 3-F picolinic acid, or pyrazine-2-carboxylic acid was fed separately into the cultures when seed culture was transferred into the fermentation medium. After cultivation at 28°C and 220 rpm for 7 days, the fermentation culture was finally centrifuged, and the supernatants were collected and extracted by an equal volume of ethyl acetate. After evaporation of the solvent, the residues were dissolved in methanol and further analyzed using HPLC or LC-HR-ESIMS as mentioned above.

Isolation of Compounds 5 and 7 and Determination of Their Structures

For the isolation of the accumulated compound **5** in WDY208 and compound **7** in WDY210, the crude extract of 4 l of WDY208 and 10 l of WDY210 fermentation liquor was separately passed through macroporous adsorptive resins, which was eluted with 30% methanol and 80% methanol. The fraction of 80% methanol was then concentrated and loaded onto a size-exclusion column packed with Sephadex LH20 (GE Healthcare) with methanol as the solvent, and fractions containing the purified target compound were collected. The purified compound **5** was resolved in CD_3OD and compound **7** in DMSO-*d*6, and both of them were characterized using NMR.

The NMR data were recorded on a Bruker Avance 500-MHz NMR spectrometer.

Compound **5**: ^{1}H-NMR, δH (500 MHz, CD_3OD), 9.49 (1H, d, 7.84, H-3), 8.96 (1H, t, 7.89, H-4), 9.34 (1H, d, 8.10, H-5), 9.07 (1H, d, 8.18, H-12), 8.37 (1H, d, 7.54, H-14), 8.15 (1H, t, 7.87, H-13). ^{13}C-NMR, δC (150 MHz, CD_3OD), 170.17 (C, C-1), 124.88 (C, C-2), 128.05 (CH, C-3), 125.58 (CH, C-4), 115.37 (CH, C-5), 151.73 (C, C-6), 143.15 (C,C-7), 146.77 (C, C-8), 109.46 (C, C-9), 140.48 (C, C-10), 166.58 (C, C-11), 120.69 (CH, C-12), 177.66 (CH, C-13), 177.64 (CH, C-14).

Compound **7**: ^{1}H-NMR, δH (500 MHz, DMSO-*d*6), 7.51 (1H, dd, 7.52, 1.61, H-3), 7.04 (1H, t, 7.76, H-4), 6.95 (1H, dd, 7.93, 1.65, H-5), 7.35 (1H, dd, 8.16, 1.23, H-12), 6.46 (1H, d, 7.87, H-13), 6.84 (1H, dd, 7.65, 1.28, H-14). ^{13}C-NMR, δC (150 MHz, DMSO-*d*6), 172.34 (C, C-1), 131.33 (C, C-2), 124.80 (CH, C-3), 127.23 (CH, C-4), 123.10 (CH, C-5), 151.98 (C, C-6), 130.73 (C,C-7), 147.66 (C, C-8), 116.43 (C, C-9), 142.56 (C, C-10), 171.57 (C, C-11), 121.88 (CH, C-12), 117.39 (CH, C-13), 118.63 (CH, C-14).

Construction of BomE, BomL, and BomM Overexpression Plasmids

The genes *bomE*, *bomL*, and *bomM* were separately amplified by high-fidelity PCR from cosmid 8D3 using primers pET28a-BomE-F/pET28a-BomE-R, pET28a-BomL-F/pET28a-BomL-R, and pET28a-BomM-F/pET28a-BomM-R. The PCR products were then cleaved by NdeI and XhoI and cloned into the NdeI/XhoI sites of pET28a to generate expression vectors pWDY205, pWDY224, and pWDY225.

Construction of the pHS_SUMO Expression Vector

A 291-bp fragment which contains the whole SUMO was amplified from genomic DNA of *Saccharomyces cerevisiae* by PCR using the primers SUMO_F/SUMO_R. PCR was performed in 20 μl of volume with 5% DMSO and KOD DNA polymerase (Toyobo). The amplification conditions were: initial denaturation at 95°C for 5 min; 30 cycles of denaturation at 95°C for 30 s; annealing at 58°C for 30 s and extension at 68°C for 30 s; and gap infilling at 68°C for 10 min. The obtained fragments were cloned into the NdeI/SacI sites of pET28a$^+$ (Novagen) using an In-fusion HD Cloning Kit (Clontech) to yield the protein overexpression vector pHS_SUMO.

Construction of BomK Overexpression Vector

To overexpress BomK, a 1,080-bp fragment which contains the whole *bomK* was amplified from cosmid 8D3 by PCR using the primers sumo-BomK-F/R. The products were cloned into the KpnI/XhoI sites of pHS_SUMO using an In-fusion HD Cloning Kit (Clontech) to yield the overexpression construct pWDY227, which was then transformed into *E. coli* BL21 (DE3) (Novagen) to generate WDY227.

Overexpression and Purification of BomE, BomL, and BomM

E. coli BL21 (DE3) cells containing pWDY205 were grown in 500 ml of super optimal broth medium supplemented with 50 mg/ml kanamycin at 37°C with shaking at 250 rpm until an A_{600} of 0.3–0.5 was reached. Protein expression was induced by addition of 0.5 mM isopropyl β-D-1-thiogalactopyranoside with further cultivation at 28°C for 4 hr. The cells were then harvested by centrifugation and frozen at −80°C. For purification of the His_6-tagged BomE protein, the cell pellet was resuspended in 40 ml of ice-cold lysis buffer (50 mM potassium phosphate, 200 mM KCl, 5 mM imidazole, pH 8.0), and disrupted by a Nano Homogenize Machine (ATS Engineering, AH100B). To separate the cellular debris from the soluble protein, the lysate was centrifuged at 12,000 rpm and 4°C for 30 min. 1 ml of Ni-nitrilotriacetic acid resin slurry (GE Healthcare) was then added to the supernatant fraction, which was contained in a small ice box, and gently stirred for 1 hr. The mixture was transferred to a disposable column and washed with 5 ml of wash buffer (50 mM potassium phosphate, 200 mM KCl, 50 mM imidazole, pH 8.0). Recombinant BomE was eluted with 5 ml of elution buffer with 300 mM imidazole. The eluted fractions were concentrated to 2.5 ml using Centrifugal Filter Units (Millipore, Regenerated Cellulose 10,000 MWCO). The protein sample was then desalted by PD-10 Columns (GE Healthcare) according to the manufacturer's instructions. The same procedure was used to purify BomL and BomM, except that BomM was overexpressed in *E. coli* BAP1 strain which contains an *sfp* gene (Pfeifer et al., 2001). BomE was stored in storage buffer (50 mM potassium phosphate, 100 mM KCl, 10% [w/v] glycerol, pH 8.0) at −80°C. BomL was stored in storage buffer (50 mM Tris-HCl, 100 mM NaCl, 10% [w/v] glycerol, pH 8.0).

Enzyme Assay of BomE

Lysine 2-aminotransferase activity was determined based on the method described previously (Soda et al., 1968). Enzyme assay of BomE activity was carried out in a 100-μl scale with 5 mM L/D-lysine, 100 mM 2-ketoglutarate, 70 μM pyridoxal phosphate, and 10 μM purified enzyme in 50 mM MOPS buffer (pH 7.2). The mixture was incubated at 30°C for 25 min. The reaction was terminated by addition of 50 μl 100% (w/v) trichloroacetic acid. Proteins were removed by centrifugation. 40 μl of the supernatant was added into 40 μl of mixture containing 40 mM o-aminobenzaldehyde, 200 mM potassium phosphate (pH 8.0) of absolute methanol. A yellow-orange dihydrochinazolinium complex was developed during incubation at 37°C for 2 hr. The detection of the substrate and product were analyzed by HPLC, which was carried out on a DIONEX system equipped with P680 HPLC pump, using a DIKMA Diamonsil C18 column (5 μm, 250 × 4.6 mm) eluted with a linear gradient from 5% B to 95% B for 5–20 min, at a flow rate of 0.5 ml/min (solvent A was H_2O and solvent B was CH_3CN), UV monitored at 450 nm. The HR-ESIMS analysis of the reactions was performed as mentioned above.

Enzyme Assay of BomL

The reaction (100 μl) contained 50 mM Tris-HCl (pH 8.0), 10 mM $MgCl_2$, 2 mM DTT, 5 mM ATP, 2 mM substrate, 2 μM BomL, and 10 μM holo-BomM. Reactions were initiated by the addition of BomL, followed by incubating at 37°C for 20 min, then quenched by flash-freezing at −80°C. The clarified supernatant was analyzed by HPLC-HR-ESIMS (resolution 100,000), which was carried out on a Hypersil GOLD C4 column (Thermo Scientific). The column was equilibrated for 5 min with 95% solvent A (H_2O, 0.1% formic acid) and 5% solvent B (CH_3CN, 0.1% formic acid) and eluted with a linear gradient from 95% A/5% B to 5% A/95% B, for 5–20 min at a flow rate of 0.2 ml/min.

Biochemical Analysis of BomK in the Cell-Free System

Approximately 1.2 g of WDY227 overexpression cultures were extracted with 1 ml of buffer containing 50 mM Tris-HCl (pH 8.0) and 50 mM NaCl. The mixture was filtrated to provide the crude enzyme. For the cell-free conversion, 50 μl of crude enzyme was added into 100 μl of BomL reaction system, incubated at 37°C with 5 mM compound **5** or **7** as substrate for 1.5 hr, using the wild-type *E. coli* BL21 (DE3) extracts as control. The reactions were quenched by adding equal volumes of methanol. The reaction products were analyzed with HPLC-HR-ESIMS as described above.

ACCESSION NUMBERS

The accession number for the A33853 biosynthetic gene cluster reported in this paper is Genbank: KR476659.

SUPPLEMENTAL INFORMATION

Supplemental Information includes three tables and five figures and can be found with this article online at http://dx.doi.org/10.1016/j.chembiol.2015.09.005.

AUTHOR CONTRIBUTIONS

Y.Y. conceived the project and designed the experiments; M.L., J.Z., and Y.Y. carried out in vivo and in vitro experiments; M.L., J.Z., Z.D., and Y.Y. analyzed the results; and Y.Y. wrote the paper.

ACKNOWLEDGMENTS

We thank Dr. Hai Deng at the University of Aberdeen for critically reading the manuscript. This work was supported by grants from "973" Program (2012CB721006) and the National Natural Science Foundation of China (31570033, 81102357).

Received: June 6, 2015
Revised: August 26, 2015
Accepted: September 10, 2015
Published: October 22, 2015

REFERENCES

Alvar, J., Velez, I.D., Bern, C., Herrero, M., Desjeux, P., Cano, J., Jannin, J., den Boer, M., and WHO Leishmaniasis Control Team. (2012). Leishmaniasis worldwide and global estimates of its incidence. PLoS One *7*, e35671.

Blanc, V., Lagneaux, D., Didier, P., Gil, P., Lacroix, P., and Crouzet, J. (1995). Cloning and analysis of structural genes from *Streptomyces pristinaespiralis* encoding enzymes involved in the conversion of pristinamycin IIB to pristinamycin IIA (PIIA): PIIA synthase and NADH:riboflavin 5′-phosphate oxidoreductase. J. Bacteriol. *177*, 5206–5214.

Bonitz, T., Zubeil, F., Grond, S., and Heide, L. (2013). Unusual N-prenylation in diazepinomicin biosynthesis: the farnesylation of a benzodiazepine substrate is catalyzed by a new member of the ABBA prenyltransferase superfamily. PLoS One *8*, e85707.

Bretschneider, T., Zocher, G., Unger, M., Scherlach, K., Stehle, T., and Hertweck, C. (2012). A ketosynthase homolog uses malonyl units to form esters in cervimycin biosynthesis. Nat. Chem. Biol. *8*, 154–161.

Bruckner, R.C., Zhao, G., Venci, D., and Jorns, M.S. (2004). Nikkomycin biosynthesis: formation of a 4-electron oxidation product during turnover of NikD with its physiological substrate. Biochemistry *43*, 9160–9167.

Buntin, K., Irschik, H., Weissman, K.J., Luxenburger, E., Blocker, H., and Muller, R. (2010). Biosynthesis of thuggacins in myxobacteria: comparative cluster analysis reveals basis for natural product structural diversity. Chem. Biol. *17*, 342–356.

Burks, E.A., Fleming, C.D., Mesecar, A.D., Whitman, C.P., and Pegan, S.D. (2010). Kinetic and structural characterization of a heterohexamer 4-oxalocrotonate tautomerase from *Chloroflexus aurantiacus* J-10-fl: implications for functional and structural diversity in the tautomerase superfamily. Biochemistry *49*, 5016–5027.

Cano-Prieto, C., Garcia-Salcedo, R., Sanchez-Hidalgo, M., Brana, A.F., Fiedler, H.P., Mendez, C., Salas, J.A., and Olano, C. (2015). Genome mining of *Streptomyces* sp. Tu 6176: characterization of the nataxazole biosynthesis pathway. Chembiochem *16*, 1461–1473.

Chappuis, F., Sundar, S., Hailu, A., Ghalib, H., Rijal, S., Peeling, R.W., Alvar, J., and Boelaert, M. (2007). Visceral leishmaniasis: what are the needs for diagnosis, treatment and control? Nat. Rev. Microbiol. *5*, 873–882.

Croft, S.L., Seifert, K., and Yardley, V. (2006a). Current scenario of drug development for leishmaniasis. Indian J. Med. Res. *123*, 399–410.

Croft, S.L., Sundar, S., and Fairlamb, A.H. (2006b). Drug resistance in leishmaniasis. Clin. Microbiol. Rev. *19*, 111–126.

Ellis, H.R. (2010). The FMN-dependent two-component monooxygenase systems. Arch. Biochem. Biophys. *497*, 1–12.

Funabashi, M., Yang, Z., Nonaka, K., Hosobuchi, M., Fujita, Y., Shibata, T., Chi, X., and Van Lanen, S.G. (2010). An ATP-independent strategy for amide bond formation in antibiotic biosynthesis. Nat. Chem. Biol. *6*, 581–586.

He, Q.L., Jia, X.Y., Tang, M.C., Tian, Z.H., Tang, G.L., and Liu, W. (2009). Dissection of two acyl-transfer reactions centered on acyl-S-carrier protein intermediates for incorporating 5-chloro-6-methyl-O-methylsalicyclic acid into chlorothricin. Chembiochem *10*, 813–819.

Hohmann, C., Schneider, K., Bruntner, C., Irran, E., Nicholson, G., Bull, A.T., Jones, A.L., Brown, R., Stach, J.E., Goodfellow, M., et al. (2009). Caboxamycin, a new antibiotic of the benzoxazole family produced by the deep-sea strain *Streptomyces* sp. NTK 937. J. Antibiot. *62*, 99–104.

Hollenhorst, M.A., Clardy, J., and Walsh, C.T. (2009). The ATP-dependent amide ligases DdaG and DdaF assemble the fumaramoyl-dipeptide scaffold of the dapdiamide antibiotics. Biochemistry *48*, 10467–10472.

Huang, T., Wang, Y., Yin, J., Du, Y., Tao, M., Xu, J., Chen, W., Lin, S., and Deng, Z. (2011). Identification and characterization of the pyridomycin biosynthetic gene cluster of *Streptomyces pyridomyceticus* NRRL B-2517. J. Biol. Chem. *286*, 20648–20657.

Huang, W., Xu, H., Li, Y., Zhang, F., Chen, X.Y., He, Q.L., Igarashi, Y., and Tang, G.L. (2012). Characterization of yatakemycin gene cluster revealing a radical S-adenosylmethionine dependent methyltransferase and highlighting spirocyclopropane biosynthesis. J. Am. Chem. Soc. *134*, 8831–8840.

Ichinose, K., Ozawa, M., Itou, K., Kunieda, K., and Ebizuka, Y. (2003). Cloning, sequencing and heterologous expression of the medermycin biosynthetic gene cluster of *Streptomyces* sp. AM-7161: towards comparative analysis of the benzoisochromanequinone gene clusters. Microbiol. *149*, 1633–1645.

Joshi, S., Rawat, K., Yadav, N.K., Kumar, V., Siddiqi, M.I., and Dube, A. (2014). Visceral leishmaniasis: advancements in vaccine development via classical and molecular approaches. Front. Immunol. *5*, 380.

Keating, T.A., Marshall, C.G., Walsh, C.T., and Keating, A.E. (2002). The structure of VibH represents nonribosomal peptide synthetase condensation, cyclization and epimerization domains. Nat. Struct. Biol. *9*, 522–526.

Kendrew, S.G., Harding, S.E., Hopwood, D.A., and Marsh, E.N. (1995). Identification of a flavin:NADH oxidoreductase involved in the biosynthesis of actinorhodin. Purification and characterization of the recombinant enzyme. J. Biol. Chem. *270*, 17339–17343.

Knerr, P.J., and van der Donk, W.A. (2012). Discovery, biosynthesis, and engineering of lantipeptides. Annu. Rev. Biochem. *81*, 479–505.

Li, L., Xu, Z., Xu, X., Wu, J., Zhang, Y., He, X., Zabriskie, T.M., and Deng, Z. (2008). The mildiomycin biosynthesis: initial steps for sequential generation of 5-hydroxymethylcytidine 5′-monophosphate and 5-hydroxymethylcytosine in *Streptoverticillium rimofaciens* ZJU5119. Chembiochem *9*, 1286–1294.

Martin, J.F., Casqueiro, J., and Liras, P. (2005). Secretion systems for secondary metabolites: how producer cells send out messages of intercellular communication. Curr. Opin. Microbiol. *8*, 282–293.

Melby, J.O., Nard, N.J., and Mitchell, D.A. (2011). Thiazole/oxazole-modified microcins: complex natural products from ribosomal templates. Curr. Opin. Chem. Biol. *15*, 369–378.

Michel, K.H., Boeck, L.D., Hoehn, M.M., Jones, N.D., and Chaney, M.O. (1984). The discovery, fermentation, isolation, and structure of antibiotic A33853 and its tetraacetyl derivative. J. Antibiot. *37*, 441–445.

Mutiso, J.M., Macharia, J.C., Kiio, M.N., Ichagichu, J.M., Rikoi, H., and Gicheru, M.M. (2013). Development of *Leishmania* vaccines: predicting the future from past and present experience. J. Biomed. Res. *27*, 85–102.

Namwat, W., Kinoshita, H., and Nihira, T. (2002). Identification by heterologous expression and gene disruption of VisA as L-lysine 2-aminotransferase essential for virginiamycin S biosynthesis in *Streptomyces virginiae*. J. Bacteriol. *184*, 4811–4818.

Nolan, E.M., and Walsh, C.T. (2009). How nature morphs peptide scaffolds into antibiotics. Chembiochem *10*, 34–53.

Okamoto, S., Taguchi, T., Ochi, K., and Ichinose, K. (2009). Biosynthesis of actinorhodin and related antibiotics: discovery of alternative routes for quinone formation encoded in the act gene cluster. Chem. Biol. *16*, 226–236.

Pfeifer, B.A., Admiraal, S.J., Gramajo, H., Cane, D.E., and Khosla, C. (2001). Biosynthesis of complex polyketides in a metabolically engineered strain of *E. coli*. Science *291*, 1790–1792.

Pigott, D.M., Bhatt, S., Golding, N., Duda, K.A., Battle, K.E., Brady, O.J., Messina, J.P., Balard, Y., Bastien, P., Pratlong, F., et al. (2014). Global distribution maps of the leishmaniases. Elife *3*, e02851.

Pulsawat, N., Kitani, S., and Nihira, T. (2007). Characterization of biosynthetic gene cluster for the production of virginiamycin M, a streptogramin type A antibiotic, in *Streptomyces virginiae*. Gene *393*, 31–42.

Ramos, J.L., Martinez-Bueno, M., Molina-Henares, A.J., Teran, W., Watanabe, K., Zhang, X., Gallegos, M.T., Brennan, R., and Tobes, R. (2005). The TetR family of transcriptional repressors. Microbiol. Mol. Biol. Rev. *69*, 326–356.

Reed, P.W., and Lardy, H.A. (1972). A23187: a divalent cation ionophore. J. Biol. Chem. *247*, 6970–6977.

Salam, N., Al-Shaqha, W.M., and Azzi, A. (2014). Leishmaniasis in the Middle East: incidence and epidemiology. PLoS Negl. Trop. Dis *8*, e3208.

Schmutz, E., Steffensky, M., Schmidt, J., Porzel, A., Li, S.M., and Heide, L. (2003). An unusual amide synthetase (CouL) from the coumermycin A1 biosynthetic gene cluster from *Streptomyces rishiriensis* DSM 40489. Eur. J. Biochem. *270*, 4413–4419.

Shibata, K., Kashiwada, M., Ueki, M., and Taniguchi, M. (1993). UK-1, a novel cytotoxic metabolite from *Streptomyces* sp. 517-02. II. Structural elucidation. J. Antibiot. *46*, 1095–1100.

Soda, K., Misono, H., and Yamamoto, T. (1968). L-Lysine:alpha-ketoglutarate aminotransferase. I. Identification of a product, delta-1-piperideine-6-carboxylic acid. Biochemistry *7*, 4102–4109.

Sommer, P.S., Almeida, R.C., Schneider, K., Beil, W., Sussmuth, R.D., and Fiedler, H.P. (2008). Nataxazole, a new benzoxazole derivative with antitumor activity produced by *Streptomyces* sp. Tu 6176. J. Antibiot. *61*, 683–686.

Steffensky, M., Li, S.M., and Heide, L. (2000). Cloning, overexpression, and purification of novobiocic acid synthetase from *Streptomyces spheroides* NCIMB 11891. J. Biol. Chem. *275*, 21754–21760.

Sucharitakul, J., Tinikul, R., and Chaiyen, P. (2014). Mechanisms of reduced flavin transfer in the two-component flavin-dependent monooxygenases. Arch. Biochem. Biophys. *555–556*, 33–46.

Taguchi, T., Okamoto, S., Hasegawa, K., and Ichinose, K. (2011). Epoxyquinone formation catalyzed by a two-component flavin-dependent monooxygenase involved in biosynthesis of the antibiotic actinorhodin. Chembiochem *12*, 2767–2773.

Taguchi, T., Yabe, M., Odaki, H., Shinozaki, M., Metsa-Ketela, M., Arai, T., Okamoto, S., and Ichinose, K. (2013). Biosynthetic conclusions from the functional dissection of oxygenases for biosynthesis of actinorhodin and related *Streptomyces* antibiotics. Chem. Biol. *20*, 510–520.

Tipparaju, S.K., Joyasawal, S., Pieroni, M., Kaiser, M., Brun, R., and Kozikowski, A.P. (2008). In pursuit of natural product leads: synthesis and biological evaluation of 2-[3-hydroxy-2-[(3-hydroxypyridine-2-carbonyl)amino] phenyl]benzoxazole-4-c arboxylic acid (A-33853) and its analogues: discovery of N-(2-benzoxazol-2-ylphenyl)benzamides as novel antileishmanial chemotypes. J. Med. Chem. *51*, 7344–7347.

Valton, J., Filisetti, L., Fontecave, M., and Niviere, V. (2004). A two-component flavin-dependent monooxygenase involved in actinorhodin biosynthesis in *Streptomyces coelicolor*. J. Biol. Chem. *279*, 44362–44369.

Valton, J., Fontecave, M., Douki, T., Kendrew, S.G., and Niviere, V. (2006). An aromatic hydroxylation reaction catalyzed by a two-component FMN-dependent monooxygenase. The ActVA-ActVB system from *Streptomyces coelicolor*. J. Biol. Chem. *281*, 27–35.

Venci, D., Zhao, G., and Jorns, M.S. (2002). Molecular characterization of NikD, a new flavoenzyme important in the biosynthesis of nikkomycin antibiotics. Biochemistry *41*, 15795–15802.

Wang, S.C., Johnson, W.H., Jr., Czerwinski, R.M., Stamps, S.L., and Whitman, C.P. (2007). Kinetic and stereochemical analysis of YwhB, a 4-oxalocrotonate tautomerase homologue in *Bacillus subtilis*: mechanistic implications for the YwhB- and 4-oxalocrotonate tautomerase-catalyzed reactions. Biochemistry *46*, 11919–11929.

Wu, Q., Liang, J., Lin, S., Zhou, X., Bai, L., Deng, Z., and Wang, Z. (2011). Characterization of the biosynthesis gene cluster for the pyrrole polyether antibiotic calcimycin (A23187) in *Streptomyces chartreusis* NRRL 3882. Antimicrob. Agents Chemother. *55*, 974–982.

Yu, Y., Duan, L., Zhang, Q., Liao, R., Ding, Y., Pan, H., Wendt-Pienkowski, E., Tang, G., Shen, B., and Liu, W. (2009). Nosiheptide biosynthesis featuring a unique indole side ring formation on the characteristic thiopeptide framework. ACS Chem. Biol. *4*, 855–864.

Zhang, Q., and Liu, W. (2013). Biosynthesis of thiopeptide antibiotics and their pathway engineering. Nat. Prod. Rep. *30*, 218–226.

Zhang, W., Ntai, I., Kelleher, N.L., and Walsh, C.T. (2011). tRNA-dependent peptide bond formation by the transferase PacB in biosynthesis of the pacidamycin group of pentapeptidyl nucleoside antibiotics. Proc. Natl. Acad. Sci. USA *108*, 12249–12253.

